

AD-A049 975

ILLINOIS UNIV AT URBANA-CHAMPAIGN

STRUCTURE AND DEFORMATION CHARACTERISTICS OF RHEOCAST METALS. (U)

DEC 77 R MEHRABIAN, S D RAMATI

DAA646-76-C-0046

F/6 13/8

UNCLASSIFIED

AMMRC-CTR-77-30

NL

1 OF 1  
AD  
A049975

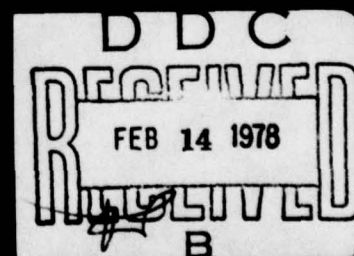


END  
DATE  
FILMED  
3 -78  
DDC

AD No. \_\_\_\_\_

JDC FILE COPY

AD A 049975



UNCLASSIFIED

SECURITY CLASSIFICATION OF THIS PAGE (When Data Entered)

REPORT DOCUMENTATION PAGE		READ INSTRUCTIONS BEFORE COMPLETING FORM
1. REPORT NUMBER <b>18</b> AMMRC CTR 77-30	2. GOVT ACCESSION NO.	3. RECIPIENT'S CATALOG NUMBER
4. TITLE (and Subtitle) <b>STRUCTURE AND DEFORMATION CHARACTERISTICS OF RHEOCAST METALS.</b>	5. TYPE OF REPORT & PERIOD COVERED Annual Report, NO 1, 24 Jun 76 - 23 Jun 77	
7. AUTHOR(s) <b>10</b> R. Mehrabian, S.D.E./Ramati, G. J. Abbaschian, D. G. Backman	6. PERFORMING ORG. REPORT NUMBER	
9. PERFORMING ORGANIZATION NAME AND ADDRESS Department of Metallurgy and Mining Engr. and Department of Mech. and Ind. Engineering University of Illinois, Urbana, IL 61801	8. CONTRACT OR GRANT NUMBER(s) <b>15</b> DAAG46-76-C-0046	
11. CONTROLLING OFFICE NAME AND ADDRESS Army Materials and Mechanics Research Center Watertown, Massachusetts 02172	10. PROGRAM ELEMENT, PROJECT, TASK AREA & WORK UNIT NUMBERS D/A Project: 1T162105AHS4 AMCMS Code: 62105A Agency Accession:	
14. MONITORING AGENCY NAME & ADDRESS (if different from Controlling Office)	12. REPORT DATE <b>17</b> Dec 1977	
	13. NUMBER OF PAGES <b>12</b> 36 p.	
	15. SECURITY CLASS (of this report) Unclassified	
16. DISTRIBUTION STATEMENT (of this Report) Approved for public release; distribution unlimited.		
17. DISTRIBUTION STATEMENT (of the abstract entered in Block 20, if different from Report) <b>DDC</b> <b>REF ID: A66110</b> <b>FEB 14 1978</b> <b>RECEIVED</b> <b>B</b>		
18. SUPPLEMENTARY NOTES		
19. KEY WORDS (Continue on reverse side if necessary and identify by block number) Rheocasting      Deformation Solidification      Forging Thixoforging		
20. ABSTRACT (Continue on reverse side if necessary and identify by block number) This is the first annual report describing research at the University of Illinois at Urbana-Champaign, aimed at establishing the feasibility of producing parts to net or near-net shapes starting with Rheocast preforms by forging-type, THIXOFORGING, operations. Ingots of Sn-15% Pb alloy and aluminum alloys 6061 and A356 were heated to temperatures above liquidus and in the liquid-solid range. The partially solidified charge, Rheocast, materials were previously made in a		

DD FORM 1473

EDITION OF 1 NOV 65 IS OBSOLETE

UNCLASSIFIED

SECURITY CLASSIFICATION OF THIS PAGE (When Data Entered)

17 5 750

JOK

UNCLASSIFIED

SECURITY CLASSIFICATION OF THIS PAGE(When Data Entered)

Block No. 20

ABSTRACT

continuous slurry producer. Sound flanged shaped cup parts with good mechanical properties and unidirectionally solidified cylinders were produced in a 50-ton hydraulic press.

Die thermal behavior was experimentally determined from thermocouples located at different distances from the metal-die interface. Measured maximum die temperatures were lower when the initial charge material was partially solid or when applied pressure was reduced. A one-dimensional computer heat flow program was developed to simulate heat flow in the cylinder parts and the steel dies. Correlation of computer predictions and measured temperatures were used to calculate values of the heat transfer coefficients at the metal-die interface prior to and after pressurization. The heat transfer coefficients increase by one order of magnitude or more upon application of  $9.1 \times 10^7$  Pa pressure. Heat transfer coefficients prior to and after pressurization were  $3.4 \times 10^3$  and  $3.4 \times 10^4 \text{ W}\cdot\text{m}^{-2}\cdot\text{K}^{-1}$ , respectively, for a liquid and  $8.4 \times 10^2$  and  $3.1 \times 10^4 \text{ W}\cdot\text{m}^{-2}\cdot\text{K}^{-1}$ , respectively, for a 0.5 volume fraction solid charge of A356 aluminum alloy.

*1 ten to the 7th power*

UNCLASSIFIED

SECURITY CLASSIFICATION OF THIS PAGE(When Data Entered)



FOREWORD

Technical monitor of the contract was Mr. R. Gagne.

This research was supported by the Army Materials and Mechanics  
Research Center, Watertown, Massachusetts, under Contract No. DAAG46-76-C-0046.

ACCESSION for		
NTIS	Wide Distribution	<input checked="checked" type="checkbox"/>
DDC	Brief Collection	<input type="checkbox"/>
UNANNOUNCED		<input type="checkbox"/>
JUSTIFICATION		
BY		
DISTRIBUTION/AVAILABILITY CODES		
Dist.	AVAIL.	and/or SPECIAL
A		

## TABLE OF CONTENTS

	Page
ABSTRACT . . . . .	1
I. INTRODUCTION . . . . .	2
II. APPARATUS AND PROCEDURE. . . . .	4
III. RESULTS AND DISCUSSION . . . . .	6
A. Cup Shaped Parts . . . . .	6
1. Partially Solid versus Liquid Charge . . . . .	8
2. Initial Die Temperature. . . . .	8
3. Applied Pressure . . . . .	8
B. Unidirectional Castings. . . . .	9
1. Thermal Measurements . . . . .	9
2. Computer Heat Flow Calculations. . . . .	9
3. Simulation Results . . . . .	11
C. Mechanical Properties. . . . .	12
IV. CONCLUSIONS. . . . .	13
V. REFERENCES . . . . .	14
APPENDIX . . . . .	16
TABLE I. . . . .	17
FIGURES. . . . .	18

## ABSTRACT

This is the first annual report describing research at the University of Illinois at Urbana-Champaign, aimed at establishing the feasibility of producing parts to net or near-net shapes starting with Rheocast preforms by forging-type, THIXOFORGING, operations.

Ingots of Sn-15%Pb alloy and aluminum alloys 6061 and A356 were heated to temperatures above liquidus and in the liquid-solid range. The partially solidified charge, Rheocast, materials were previously made in a continuous slurry producer. Sound flanged shaped cup parts with good mechanical properties and unidirectionally solidified cylinders were produced in a 50 ton hydraulic press.

Die thermal behavior was experimentally determined from thermocouples located at different distances from the metal-die interface. Measured maximum die temperatures were lower when the initial charge material was partially solid or when applied pressure was reduced. A one dimensional computer heat flow program was developed to simulate heat flow in the cylindrical parts and the steel dies. Correlation of computer predictions and measured temperatures were used to calculate values of the heat transfer coefficients at the metal-die interface prior to and after pressurization. The heat transfer coefficients increase by one order of magnitude or more upon application of  $9.1 \times 10^7$  Pa pressure. Heat transfer coefficients prior to and after pressurization were  $3.4 \times 10^3$  and  $3.4 \times 10^4 \text{ W}\cdot\text{m}^{-2}\cdot\text{K}^{-1}$ , respectively, for a liquid and  $8.4 \times 10^2$  and  $3.1 \times 10^4 \text{ W}\cdot\text{m}^{-2}\cdot\text{K}^{-1}$ , respectively, for a 0.5 volume fraction solid charge of A356 aluminum alloy.



## I. INTRODUCTION

Fundamental and applied research in the past five years has led to the finding that certain metal forming operations can be carried out using a partially solid charge material provided the solid present is particulate and spheroidal in shape; it is non-dendrite [1-5]. In the work presented here, the possibility of exploiting the special metallurgical structure and rheological behavior of a partially solidified alloy in a forging-type operation was investigated, and the results were compared to conventional liquid metal forging. The effect of process variables during forging of both liquid and partially solid aluminum alloys on the structure and properties of components produced and on the die thermal behavior was studied. Computer simulation work on heat flow was carried out to determine the effect of applied pressure during the forging operation on the heat transfer coefficient at the die-metal interface.

Shaping of liquid metals by forging-type operations has been described under a variety of names such as squeeze casting, liquid metal forging, extrusion casting and liquid stamping. The basic process steps are as follows. A measured amount of liquid metal is poured into the lower cavity of an open die set. After partial solidification of the outer extremity of the charge, the two die halves are brought together to form the part. Solidification is then completed under a predetermined hydrostatic pressure. While the process is relatively new in the U.S.A., it had been extensively investigated and used in the U.S.S.R. and to a lesser degree in Japan.

Various investigators have reported substantial improvements in microstructure (e.g., porosity) and mechanical properties over conventional castings when solidification is carried out under a direct applied pressure. Plyatskii



[6] has reported improvements in bend and tensile strengths of cast iron solidified under a pressure of  $\sim 2 \times 10^6$  Pa. Nishida and Suzuki [7] studied the effect of applied pressure on gas porosity in aluminum castings and report that a pressure of  $\sim 5 \times 10^7$  Pa resulted in complete disappearance of all macroscopic porosity. They attribute this observation to increased solubility of hydrogen in the solid with increasing applied pressure. Suzuki, et al. [8-11] have reported significant improvements in tensile and impact strength, ductility, fatigue and wear properties of Al-(2-22%)Si alloys solidified under pressures of up to  $\sim 3 \times 10^8$  Pa. Similar results were obtained in other aluminum alloys [12] and copper base alloys [13, 14]. Other investigators have reported increased solid solubility of Si in aluminum [15, 16] and changes in solidification temperature range [7, 16-19] due to the applied pressure. Shorter local solidification times due to an increase in metal-die heat transfer coefficient with applied pressure has also been postulated [20].

Shaped components of a variety of alloys including aluminum, copper and steel alloys have been produced via liquid metal forging. Plyatskii [6] has reported production of drill bit collars, engine compressor parts and turbine blades. Bidulya, et al. [21, 22] have discussed the process variables in production of a 321 stainless steel hub ( $\sim 52$  Kg) and various modes of die failure. Recent work in production of shaped parts in the U.S.A. has also been reported [23-25].

The important liquid forging process parameters noted in the above studies include the following:

- (a) melt and die temperatures;
- (b) die material and die coating;
- (c) dwell time of charge in the die before pressurization; and
- (d) magnitude and duration of applied pressure.

A common feature of the various techniques used in producing shaped components via liquid forging is partial solidification of the charge in the die cavity prior to application of pressure. Earlier fundamental studies on partially solid metal slurries has shown that the structure, viscosity and thixotropic behavior of these materials can be especially designed by proper manipulation of process variables during slurry production [4]. The thixotropic behavior of the partially solid charge should reduce metal handling, transfer and metering problems normally associated with liquid forging. Furthermore, the shear rate dependence of charge viscosity should permit development of a net shape forming process more akin to solid metal forging processes under significantly reduced applied pressures.

While it is generally recognized that pressurization during solidification enhances heat transfer across a metal-die interface, little experimental and theoretical work has been carried out to investigate this phenomenon. The heat transfer coefficient would affect die thermal behavior, hence die failure, in important ways. In the work described herein thermal data obtained from thermocouples located in the die and forgings were combined with a one-dimensional computer heat flow model to determine the effect of applied pressure on the aluminum alloy - steel die heat transfer coefficients.

## II. APPARATUS AND PROCEDURE

The apparatus for forging of liquid and partially solid charge materials, shown in Figure 1, consists of: (a) a resistance furnace; (b) a controlled pressure penetrometer for monitoring the charge material characteristics; (c) a 50 ton Wabash hydraulic press containing a controlled temperature die set; and (d) temperature measurement and control devices.



The resistance furnace for reheating, partial or complete melting, of the charge material is shown on the left side of Figure 1(a) and consists of a vertical cylindrical chamber, 0.06 m in diameter and 0.12 m long. Its temperature is controlled to  $\pm 1^{\circ}\text{K}$ . The charge material located in an alumina crucible can be moved out of the furnace by a hydraulic jack located below it. The penetrometer consists of a  $3.2 \times 10^{-3}$  m diameter alumina rod attached at one end to a small air cylinder. The lower end of the penetrometer rests on top of a slug of the charge material and exerts a controlled amount of pressure on the slug. It is calibrated to penetrate slugs of partially solid materials at a given velocity when the slugs reach a desired volume fraction solid during the heating cycle. Calibration, pressure setting, was done by locating two thermocouples in the slug, one near the center and one close to the edge. During reheating cycle of the various partially solid charge materials, the penetrometer was the primary control for determining when the charge was ready for the forging operation. The temperature in superheated liquid charge materials was monitored by a thermocouple located in the alloy. Once a charge material was deemed ready for the forging operation, it was manually transferred to the lower cavity of the die in the hydraulic press.

The H-19 steel dies were used to produce a flanged cup shaped part and a unidirectionally solidified cylindrical shaped part, see Figure 2. The dies were preheated to the desired temperature via six 1000 watt cartridge heaters located in the lower die, and a smaller heater snugly fitted inside the upper die. Die temperature was closely controlled via a control device coupled to the heaters. An H-13 steel ejector cylinder was machined and located at the bottom of the lower die. Thermocouples were press fitted in this piece at distances of  $10^{-3}$ ,  $9 \times 10^{-3}$  and  $15 \times 10^{-3}$  meters from the metal-die interface.

The charge materials used were a model low temperature Sn-15%Pb alloy and two commercial aluminum alloys; 6061 and A356. The alloys for forging in the liquid-solid range were prepared in a continuous slurry production (rheocasting) machine previously described [2, 5].

The die coating used for the tin-lead alloys was molybdenum disulfide aerosol spray, while an oil graphite mixture was generally used for the aluminum alloys. In the unidirectional solidification experiments, the sides of the lower die and the bottom of the top die were lined with fiberfrax paper and cement. Two or three thermocouples were located inside the cavity at various distances from the metal-die interface, see Figures 2(c) and 2(d).

The volume of the charge material in each experiment was  $85 \times 10^{-6} \text{ m}^3$ . After introduction of the charge in the lower die half, the dies were closed at a speed of  $\sim 0.018 \text{ m/sec}$ . The process variables studied were temperature or volume fraction solid of the charge material, die temperature and applied pressure. Due to the speed limitations of the present apparatus, no special effort was made to study the effect of shear strain and dwell time. Two types of parts were produced, a flanged cup and a unidirectionally solidified cylinder.

Parts produced were subjected to normal metallographic examination. Several tensile specimens were machined from the 6061 aluminum alloy flanged cups. These were heat treated, solutionized 13 hours at  $520^\circ\text{C}$  and aged 8 hours at  $175^\circ\text{C}$ , and tested for tensile properties.

### III. RESULTS AND DISCUSSION

#### A. Cup Shaped Parts

Figure 3 shows photographs and a representative microstructure of Sn-15%Pb alloy part. The volume fraction of solid,  $g_s$ , in the initial charge was  $\sim 0.5$  -- its temperature was  $465^\circ\text{K}$ . The larger spheroidal particles in Figure



3(b) were those existing in the charge prior to pressurization. The darker matrix is the eutectic liquid that solidified last. The measured temperature profiles in the die, at  $10^{-3}$  m from the metal-die interface, are shown in Figure 4. In order to distinguish between forgings produced from completely liquid and partially solid initial charge materials, the latter will hereafter be referred to as thixoforging -- forging of a thixotropic charge material.

The microstructures of flanged cups produced from partially solid and liquid 6061 aluminum alloy charge materials are shown in Figure 5. Figure 5(a) shows the characteristic structure of a thixoforged material. Each grain resulted from coarsening of a primary solid particle in the initial slurry. The dendritic structure of Figure 5(b) is that expected from conventional solidification of a completely liquid charge.

The thermal response of the dies as a function of the time during forging of liquid and partially solid 6061 aluminum alloy is shown in Figure 6. For each charge material, the die temperature increases as soon as the metal is poured into the die cavity. For the thermocouple located at  $10^{-3}$  m from the die surface, the rate of temperature increase rises sharply when the dies close and the pressure builds up. The pressurization times, about 8 seconds after pouring, are shown by the arrows in Figure 6. The die temperature further increases after pressurization until a maximum is reached, then it drops. The thermocouples located at  $5 \times 10^{-3}$  and  $9 \times 10^{-3}$  m respond similarly; however, their response is considerably slower and they do not show the sharp change in temperature profile at the pressurization time. Furthermore, the maximum temperature attained at each thermocouple decreases as the distance from the interface increases. The temperatures of all the thermocouples eventually become the same and then gradually decrease to the initial die temperature

of  $\sim 673^{\circ}\text{K}$ . Finally, the rate and amount of the temperature increase of the die depends on the process variables and on the nature of the charge, as discussed below.

### 1. Partially Solid versus Liquid Charge

The measured die temperatures during production of flanged cup parts of Sn-15%Pb alloy and 6061 aluminum alloy are shown in Figures 4 and 6, respectively. The lower die temperatures recorded when partially solid charge materials were used are due to their lower temperatures and heat contents.

### 2. Initial Die Temperature

The effect of initial die temperature on thermal profiles during the casting cycle were investigated. It was found that the relative change in die temperature could be lowered by increasing the initial die temperature. The limitations of the press speed in the apparatus necessitated the use of relatively high initial die temperatures (about  $673$  to  $773^{\circ}\text{K}$  for the aluminum alloys).

### 3. Applied Pressure

The effect of applied pressure on die thermal behavior was studied on superheated ( $50^{\circ}\text{K}$ ) 6061 aluminum alloy charge material. Figure 7 shows results obtained with die pressures of  $6.1 \times 10^7$  and  $13.7 \times 10^7$  Pa, respectively. As expected, increasing the applied pressure increased the heat transfer coefficient at the metal-die interface, resulting in a corresponding increase in recorded die temperatures. However, the effect of increased pressure on die thermal response is expected to level off at higher pressures. It should be noted that measured maximum die temperatures in Figure 7 are lower than those shown in Figure 6. This apparent contradiction is due to variations of the process variables in these two sets of experiments, i.e., initial die temperatures and different die coatings.

## B. Unidirectional Castings

A set of unidirectional heat flow experiments were carried out with the A356 aluminum alloy. These were specifically designed to permit determination of heat transfer coefficients at the metal-die interface using a one-dimensional computer heat flow model. All process variables except those noted in the figures were kept constant during these experiments.

### 1. Thermal Measurements

A typical example of measured temperature profiles in both the thixoforging and the die are shown in Figure 8. The vertical arrow in this figure indicates time of pressurization. Thermocouple locations are shown in the schematics of Figure 2(c) and (d). The thermocouples located near the forging-die interface (on both sides of the interface) show a rapid response to pressurization. The die thermocouple recorded a rapid temperature increase while the thermocouples located in the forging responded by a corresponding temperature decrease after a short delay time. Slopes of the temperature curves were measured using an expanded time scale like that shown in Figure 9. It was found that the rates of temperature change with time in the die thermocouple, located at 1 mm, were  $2^{\circ}\text{K/sec}$  and  $22^{\circ}\text{K/sec}$  before and after pressurization.

The die thermal behavior, at the given applied pressure, for liquid and partially solid charge materials was determined, Figure 9. The die thermal response to the liquid charge is more pronounced. The microstructures of these two castings are shown in Figure 10. No porosity was observed in these components at a magnification of 250X -- the dark spots on the photomicrographs are etching effects.

### 2. Computer Heat Flow Calculations

A unidirectional computer heat flow program similar to that previously reported [26] was developed to permit indirect determination of heat transfer



coefficients prior to and after pressurization of different charge materials. The geometry, dimensions, and coordinate system of both the computer model and the forging design are shown in Figure 11. The computer program employs a finite one dimensional model of the general heat flow equation which is solved using a forward difference technique.

A number of physical assumptions have been incorporated in the heat flow model to simplify the solution of the problem. They are:

- 1) The die is filled instantaneously.
- 2) When employed, pressurization commences instantaneously after a fixed, finite time following die filling.
- 3) The die is initially at uniform temperature and undergoes no solid state transformations upon heating.
- 4) The physical properties of liquid metal are independent of temperature.
- 5) Heat flow at the metal-die interface is characterized by a surface heat transfer coefficient,  $h$ , which changes only at the time of pressurization.
- 6) Convective cooling of the die assembly at the outer die surface is governed by a heat transfer coefficient,  $h_b$ , which is independent of time.

The mathematical problem can be represented by the one dimensional thermal diffusion equation:

$$k \frac{\partial^2 T}{\partial x^2} = \frac{\partial H}{\partial t} \quad (1)$$

where  $H$ ,  $T$ ,  $t$ , and  $k$  represent the enthalpy, temperature, time and thermal conductivity, respectively. The boundary and initial conditions employed are:



$$1) \quad x = L_C; \frac{\partial T}{\partial x} = 0 \quad (\text{from symmetry})$$

$$2) \quad x = -L_D; \frac{\dot{Q}}{A} = h_B \Delta T_B$$

$$3) \quad x = 0; \frac{\dot{Q}}{A} = h \Delta T_S$$

$$4) \quad t = 0, 0 < x < L_C; T = T_0$$

$$5) \quad t = 0, -L_D < x < 0; T = T_D$$

where  $T_D$  and  $T_0$  are the initial die and metal temperatures, respectively, and  $\Delta T_B$  and  $\Delta T_S$  are the temperature differences across the outer die surface and the metal-die interface. The ratios  $\dot{Q}/A$  represent the rate of heat flow through a perpendicular surface of unit area.  $L_D$  and  $L_C$  are the die thickness and forging half thickness, respectively. Each of the above parameters are shown in Figure 11.

The computer program employs these equations and the boundary conditions reduced to finite difference form. In addition, the program incorporates functions which interrelate temperature and enthalpy for both the steel die and the A356 aluminum alloy. The details of these features are presented in the Appendix. Finally, the computer program was processed using an IBM 360 digital computer.

### 3. Simulation Results

Numerous thermal simulations were conducted in order to obtain agreement between the computer predicted temperature curves and the experimentally determined temperature profiles. In order to accomplish this, it was necessary to abruptly alter the value of the interface heat transfer coefficient,  $h$ , at the time of pressurization. The results of the thermal

simulation are compared with the experimentally measured temperatures in Figures 12 and 13 for the forging of fully liquid and partially solid (volume fraction solid  $\sim 0.5$ ) A356 aluminum alloy.

For the fully liquid metal, the agreement between the two sets of curves is good, particularly at 1 and 9 mm from the interface, see Figure 12. The two values of the interface heat transfer coefficient,  $h_I$  and  $h_{II}$ , applicable before and after pressurization, respectively, were  $3.4 \times 10^3 \text{ W.m}^{-2}\text{K}^{-1}$  and  $3.4 \times 10^4 \text{ W.m}^{-2}\text{K}^{-1}$ . Similarly, for the partially solid aluminum alloy, the agreement between the measured and simulated profiles is good for times less than  $\sim 27$  seconds, see Figure 13. For this case, the values of  $h_I$  and  $h_{II}$  are  $8.4 \times 10^2 \text{ W.m}^{-2}\text{K}^{-1}$  and  $3.1 \times 10^4 \text{ W.m}^{-2}\text{K}^{-1}$ . For longer times it was difficult to maintain good agreement between experiment and simulation due to radial heat losses in the die which could not be incorporated in the one dimensional model.

For both casting simulations, Figures 12 and 13, the onset of pressurization is accompanied by at least an order of magnitude increase in the value of the interface heat transfer coefficient. This finding reflects the increased contact area between the charge and the die as the pressure across the interface is increased. Similarly, the initial value of the interface heat transfer coefficient,  $h_I$ , for the partially solid charge is only 25% of the value of  $h_I$  applicable during the forging of fully liquid metal. The reduced value of  $h_I$  for the partially solid charge is due its higher viscosity, and hence reduced contact area prior to pressurization.

### C. Mechanical Properties

Flanged cup parts made from both liquid and partially solid 6061 aluminum alloy charge material were sectioned, heat treated and tested for tensile



properties. Average tensile data from several specimens are listed in Table I. These data show that even with the limitations of the hydraulic press used, the parts made can be heat treated and possess relatively good tensile properties.

### CONCLUSIONS

1. The feasibility of producing parts from a partially solid thixotropic charge material in a forging-type operation was demonstrated. Flanged cup shaped parts were produced from both liquid and partially solid Sn-15%Pb and aluminum alloy charge materials.

2. Die thermal response to solidification under pressure was studied under a variety of processing conditions. A one-dimensional computer heat flow model was developed and used to correlate measured temperature profiles with predictions based on various metal-die heat transfer coefficients.

3. Relative rise in die temperature increases with increasing initial charge temperature and with increasing applied pressure.

4. There is an abrupt change in the metal-die heat transfer coefficient due to pressurization. Applied pressure of  $9.1 \times 10^7$  Pa increases the heat transfer coefficient of an aluminum alloy liquid charge material from  $3.4 \times 10^3 \text{ W.m}^{-2}\text{K}^{-1}$  to  $3.4 \times 10^4 \text{ W.m}^{-2}\text{K}^{-1}$ . The corresponding change for a partially solid initial charge material is  $8.4 \times 10^2 \text{ W.m}^{-2}\text{K}^{-1}$  to  $3.1 \times 10^4 \text{ W.m}^{-2}\text{K}^{-1}$ .

V. REFERENCES

1. M. C. Flemings and R. Mehrabian, Trans. AFS 81, 81 (1973).
2. R. G. Riek, A. Vrachnos, K. P. Young, N. Matsumoto and R. Mehrabian, Trans. AFS 83, 25 (1975).
3. R. Mehrabian and M. C. Flemings. New Trends in Materials Processing. Metals Park, Ohio: American Society for Metals, 1976, 98.
4. P. A. Joly and R. Mehrabian, J. Matl. Sci. 11, 1363 (1976).
5. R. Mehrabian, D. G. Backman, Y. V. Murty, S. Hong and C. Levi, SDCE Transactions, Paper No. G-T77-093, 1977.
6. V. M. Plyatskii. Extrusion Casting. New York: Primary Sources, 1965.
7. N. Nishida and S. Suzuki, Light Metals (Japan) 20, 628 (1972).
8. S. Suzuki, M. Ochiai, M. Ito, I. Shirayanagi and T. Awano, Tech. Reports at Nagoya Tech. Inst. 10, 299 (1961).
9. S. Suzuki, M. Ochiai, I. Shirayanagi, M. Ito, S. Kurhashi and T. Awano, Tech. Reports at Nagoya Tech. Inst. 11, 610 (1962).
10. S. Suzuki, M. Ochiai, M. Ito, I. Shirayanagi, S. Kurhashi and T. Awano, Tech. Reports at Nagoya Tech. Inst. 12, 517 (1963).
11. S. Suzuki, M. Ochiai, M. Ito, I. Shirayanagi, N. Izawa and K. Aoki, Tech. Reports at Nagoya Inst. 14, 159 (1965).
12. S. Oya, Y. Matsuura, S. Suzuki and E. Nakata, Light Metals (Japan) 23, 345 (1972).
13. S. Oya, Y. Matsuura and A. Kamio, J. Japan Foundrymen's Soc. 40, 8 (1968).
14. S. Oya, Y. Matsuura, S. Suzuki and A. Kamio, J. Japan Foundrymen's Soc. 41, 29 (1969).
15. J. L. Reiss and E. C. Kron, Mod. Castings, 89 (March, 1960).
16. I. Fujishiro, et al., J. Materials (Japan) 20, 952 (1971).
17. A. Suzuki and J. Nakamura, J. Japan Inst. Metal 33, 830 (1969).
18. A. Suzuki, J. Nakamura and T. Sakamoto, Trans. Japan Inst. Metal 33, 834 (1969).
19. S. Oya, Y. Matsuura, T. Takada, A. Kamio and E. Ozawa, Limited Metals (Japan) 18, 377 (1968).



20. N. Kagiwada and Y. Nakagawa, Tetsu to Hagane (Iron and Steel, Japan) 52, 454 (1966).
21. P. N. Bidulya and V. N. Zlodeev, Russian Casting Production, 195 (April, 1967).
22. N. A. Kudrin and P. N. Bidulya, Russian Casting Production, 31 (September, 1972).
23. R. F. Lynch, R. P. Olley and P. C. J. Gallagher, Paper No. 75-90, 79th AFS Casting Congress (May, 1975).
24. R. F. Lynch, R. P. Olley and P. C. J. Gallagher, Paper No. 75-122, 79th AFS Casting Congress (May, 1975).
25. D. A. Stawarz, K. M. Kulkarni, R. B. Miclot and K. R. Iyer. Technical Report of AMDRC, Contract DAAF03-73-C0099, Rock Island, Illinois (September 1976).
26. D. G. Backman, R. Mehrabian and M. C. Flemings, to be published in Met. Trans. B.

## APPENDIX

Values of Material Properties Used  
in the Computer SimulationDensity

The values of density for the H-13 or 19 steel die and the aluminum alloys are 7800 and 2700 kg/m<sup>3</sup>.

Thermal  
Conductivity

Steel = 33.5 watt/m<sup>0</sup>K

Aluminum = 167.4 watt/m<sup>0</sup>K

Enthalpy

The variation of enthalpy, H in cal/gm, with temperature for both the steel die and the aluminum was represented by a series of linear approximations.

Steel            H = 0.163T - 6.231

Aluminum A356 H = 0.258T - 12.890

T < 835<sup>0</sup>K

H = 2.200T - 1104.400

835<sup>0</sup>K < T < 885<sup>0</sup>K

H = 0.262T + 81.384

T > 885<sup>0</sup>K

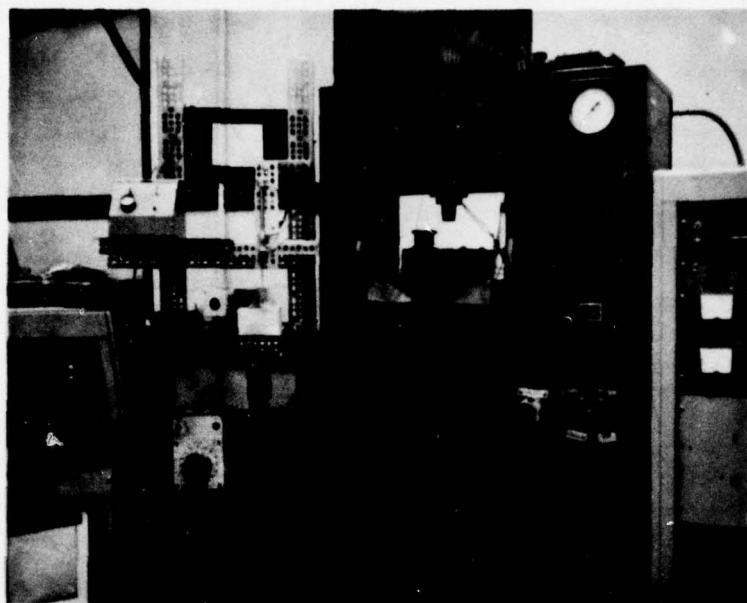
TABLE I  
Tensile Properties of Heat Treated  
6061 Aluminum Alloy Flanged Cup Parts\*

Charge	Die Temp. °K	Y.S. (MPa)	UTS (MPa)	% Elongation**
Original Rheo-cast Ingot		165	207	4
Thixoforged	723	152	214	7
Thixoforged	773	172	252	18.5
Liquid (50°K Superheat)	773	200	252	9

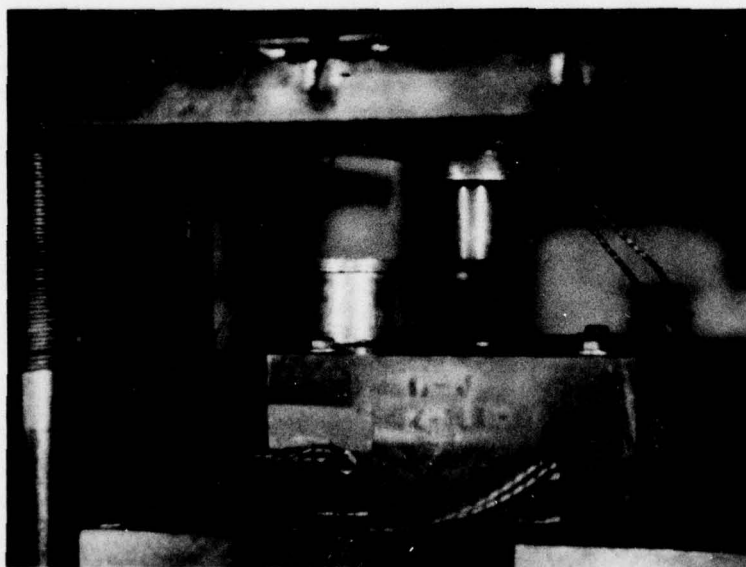
\* Die pressure of  $9.1 \times 10^7$  Pa (30 tons).

\*\* in 1.3 cm section.





[a]



[b]

Figure 1 Photographs of apparatus for forging of partially solidified alloys into shapes. (a) Overall view of the apparatus including slug reheating furnace, penetrometer, hydraulic press, and controllers, (b) the two die halves and the flanged cup produced.

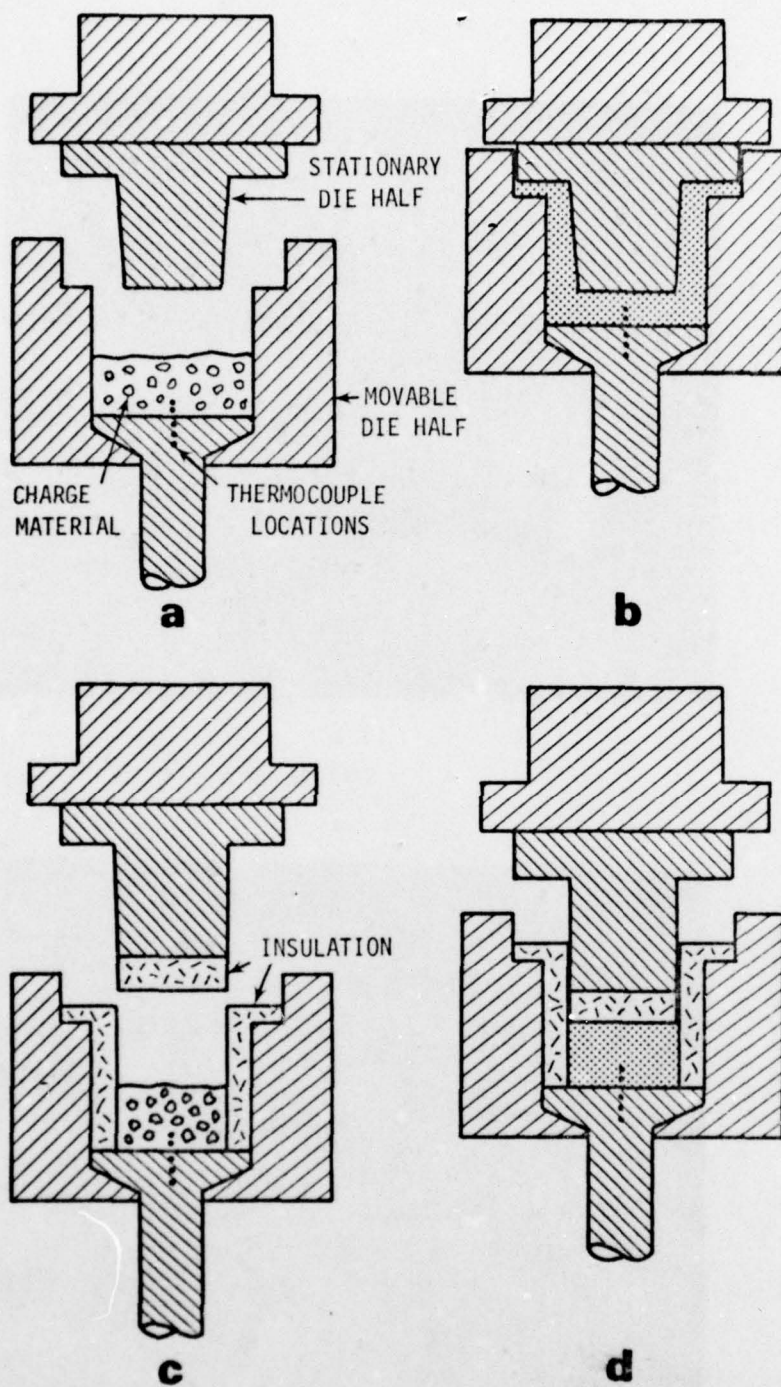
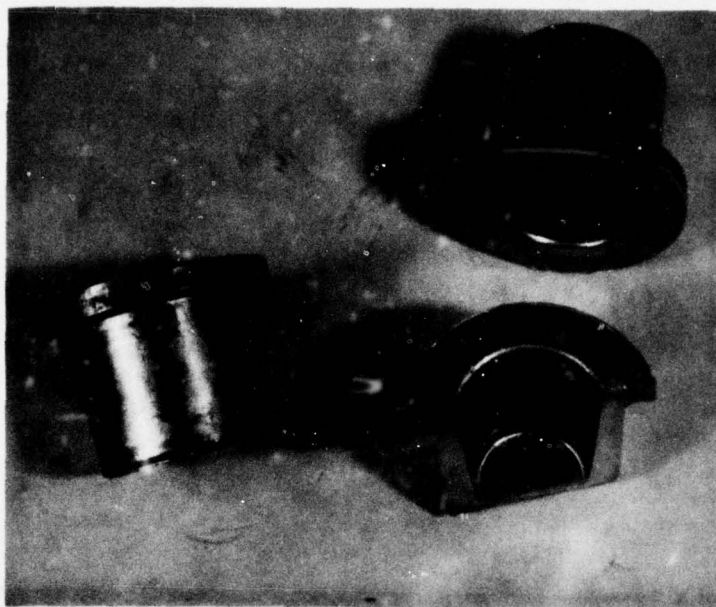
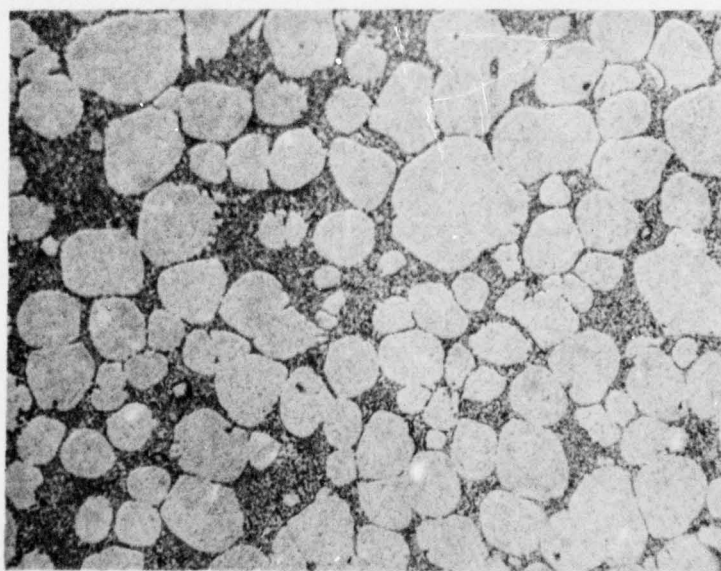


Figure 2. Schematic illustration of dies used in the forging apparatus; (a) and (b) refer to the cup shaped part, (c) and (d) refer to the uni-directionally solidified cylinders.



[a]



[b]

Figure 3 Photograph and a representative microstructure of Sn-15% Pb flanged cup parts. The volume fraction of solid in the initial charge was  $\sim 0.5$ . (a) Photograph of two complete parts and a longitudinally sectioned part, (b) Internal microstructure at 100X.



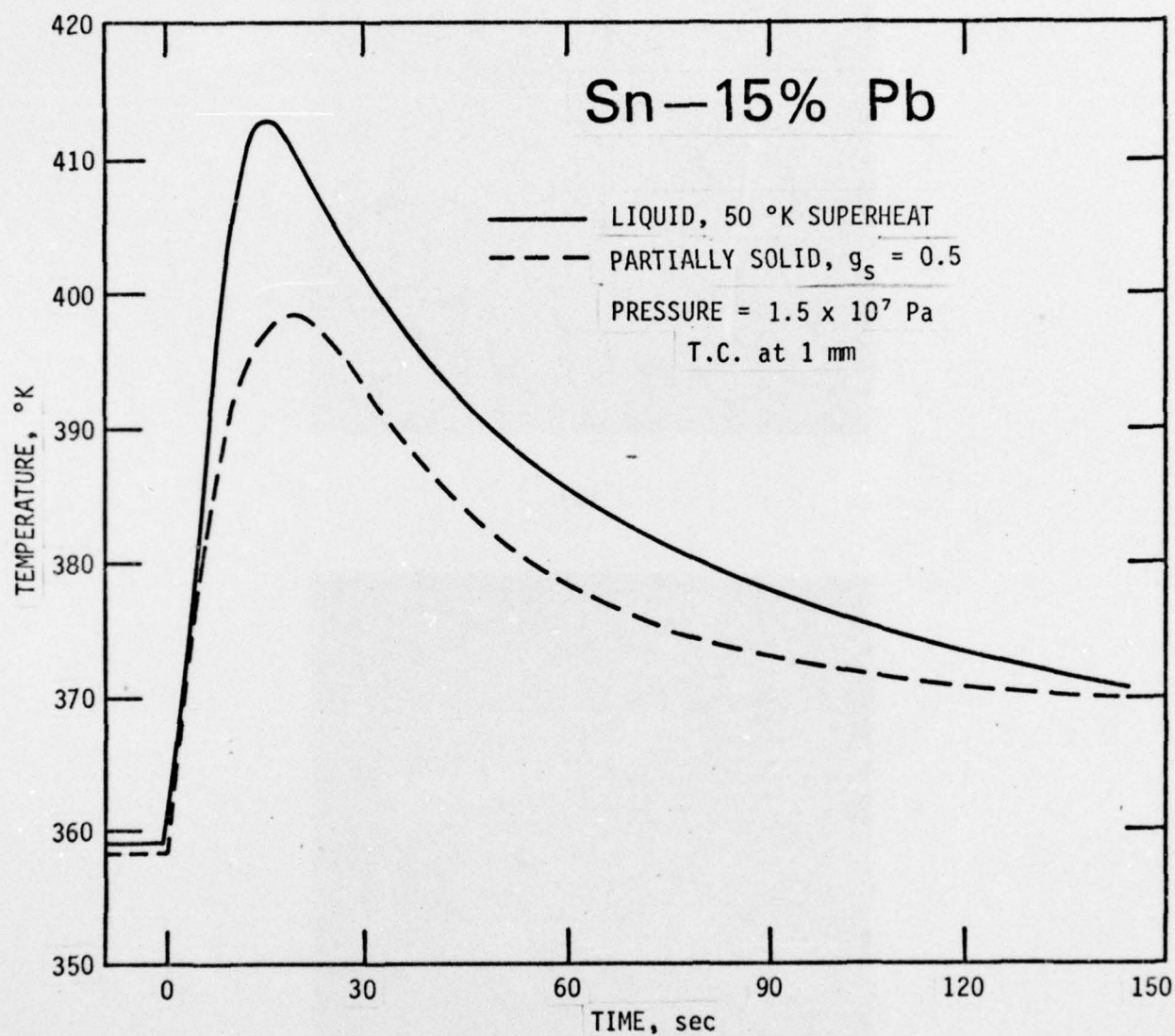
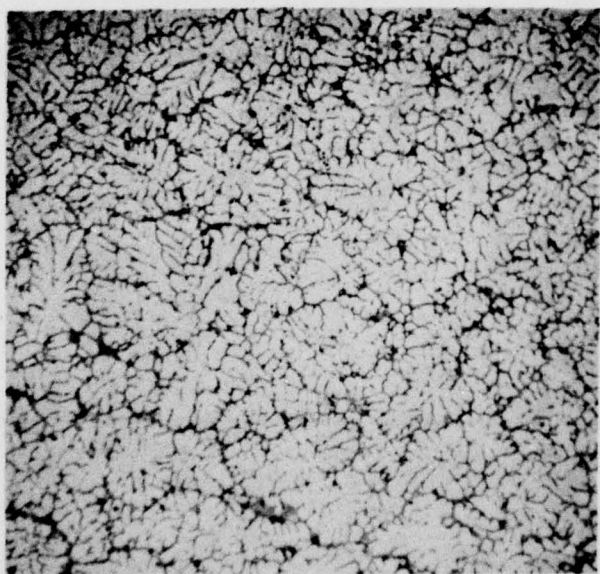


Figure 4. Die surface thermal response -- comparison between a superheated liquid and a partially solid initial charge. Flanged cup die cavity.



[a]



[b]

Figure 5 Microstructures of 6061 aluminum alloy parts at 55X magnification. (a) Thixoforged part at volume fraction solid of  $\sim 0.65$ , (b) Part made with a completely liquid initial charge.

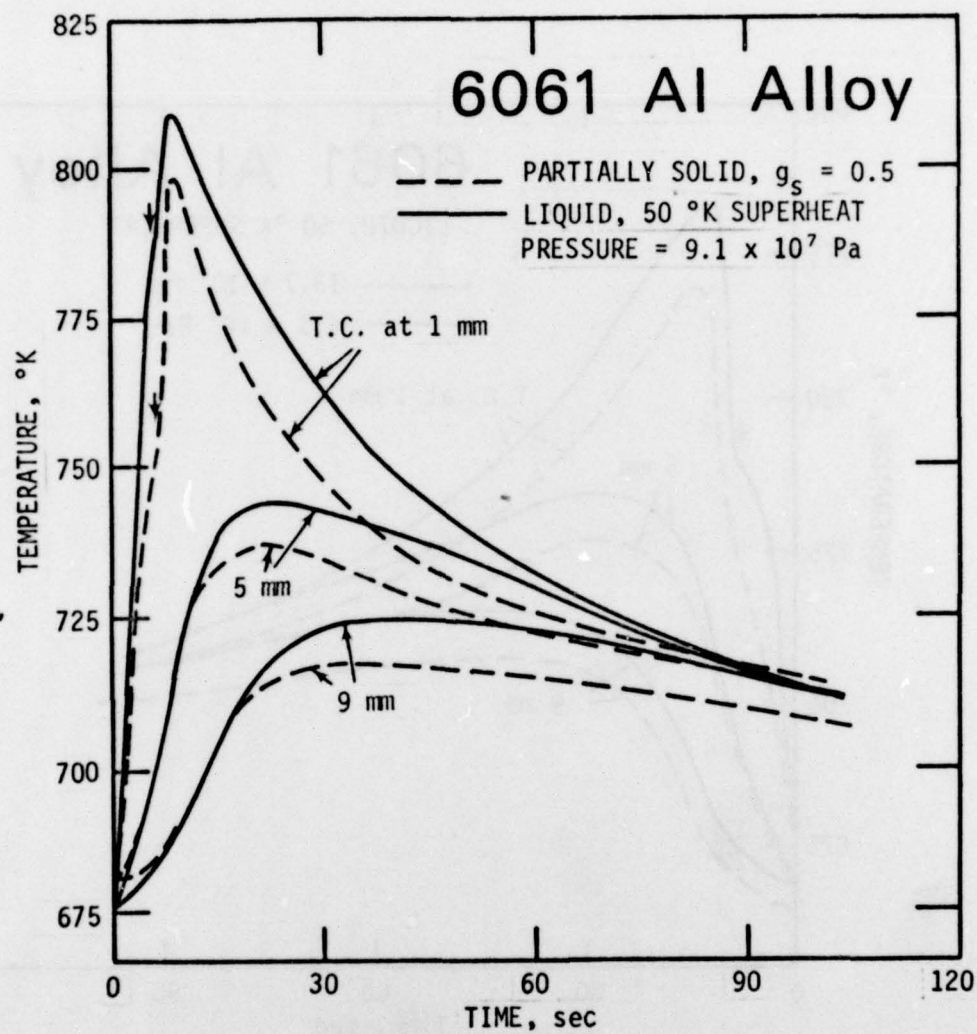


Figure 6. Die thermal response -- comparison between a superheated liquid and a partially solid initial charge. Flanged cup die cavity.



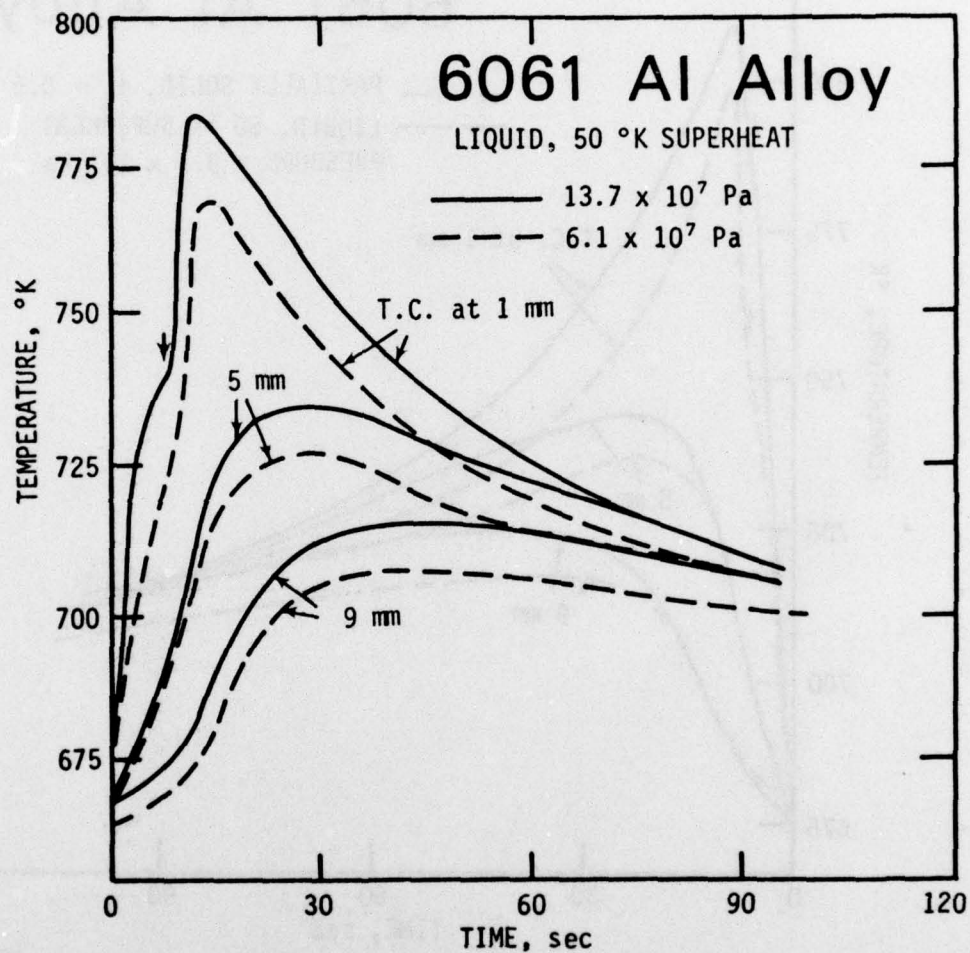


Figure 7. Effect of pressure on die thermal response during liquid forging. Note  $13.7 \times 10^7$  and  $6.1 \times 10^7$  Pa correspond to 20 and 45 tons in the hydraulic press, respectively. Flanged cup die cavity.

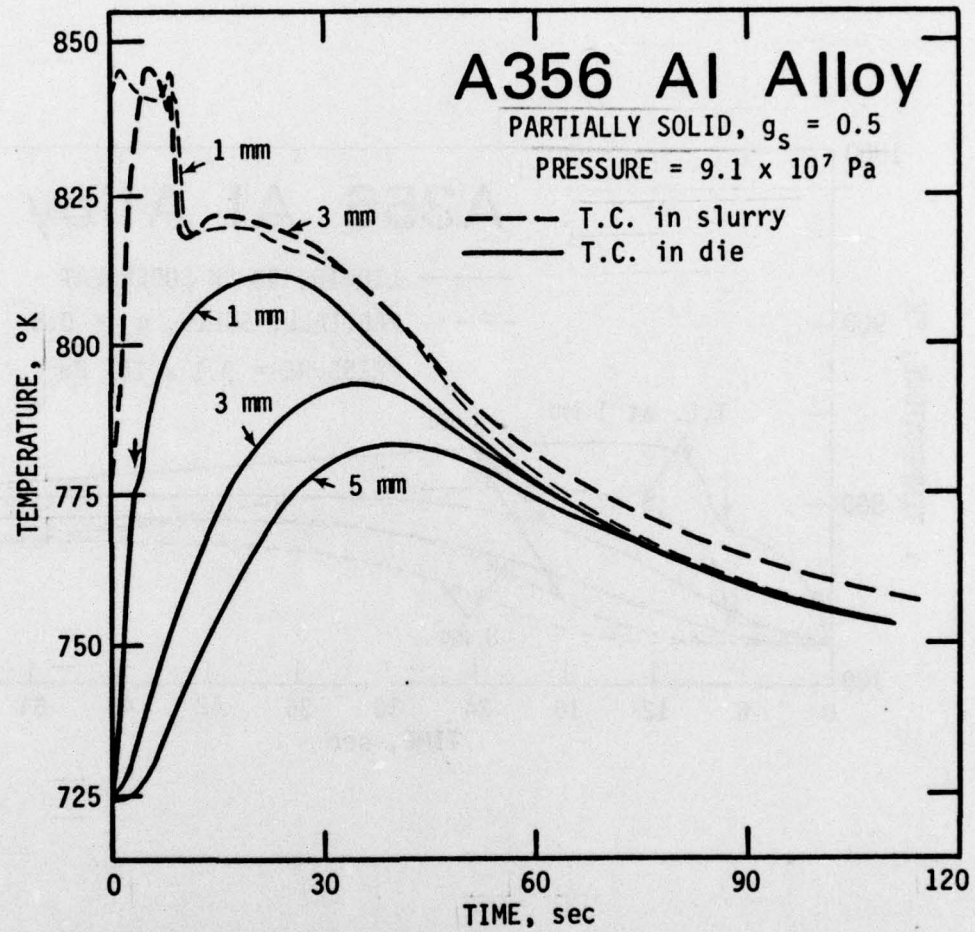


Figure 8. Composite of die and forging thermal response. Unidirectional die cavity.

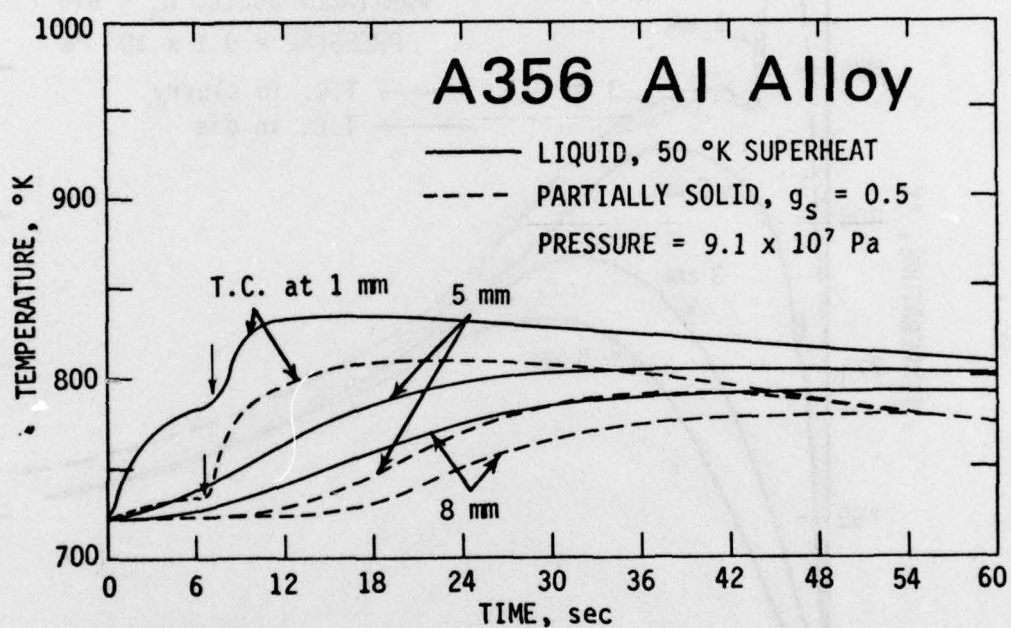
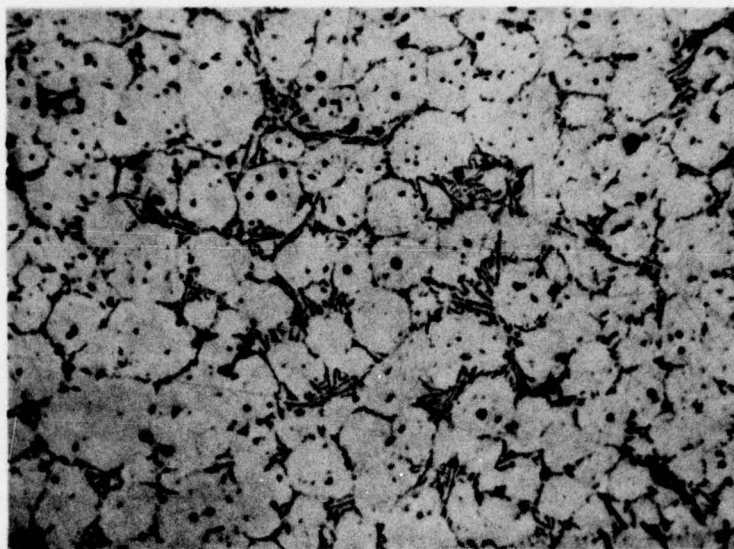
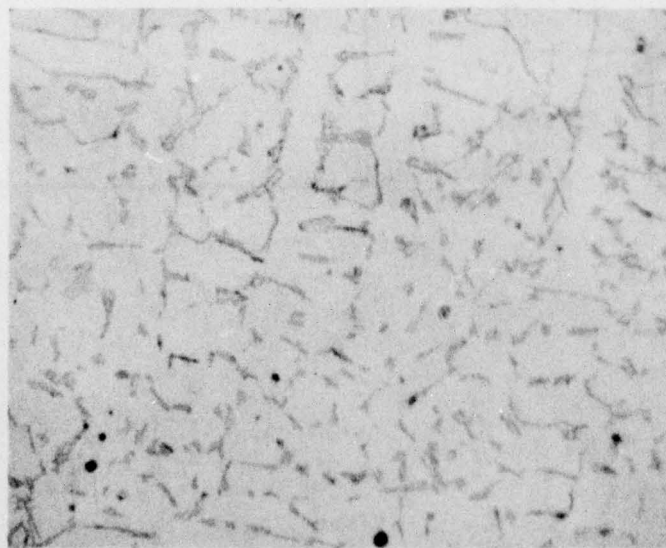


Figure 9. Die thermal response -- comparison between a superheated liquid and a partially solid initial charge. Unidirectional die cavity.





[a]



[b]

Figure 10 Microstructures of A356 aluminum alloy forgings made in the unidirectional die cavity. Magnification 100X. (a) Thixoforged part--initial volume fraction solid  $\sim 0.6$ , (b) Part made from a superheated ( $\sim 50^\circ\text{K}$ ) liquid.

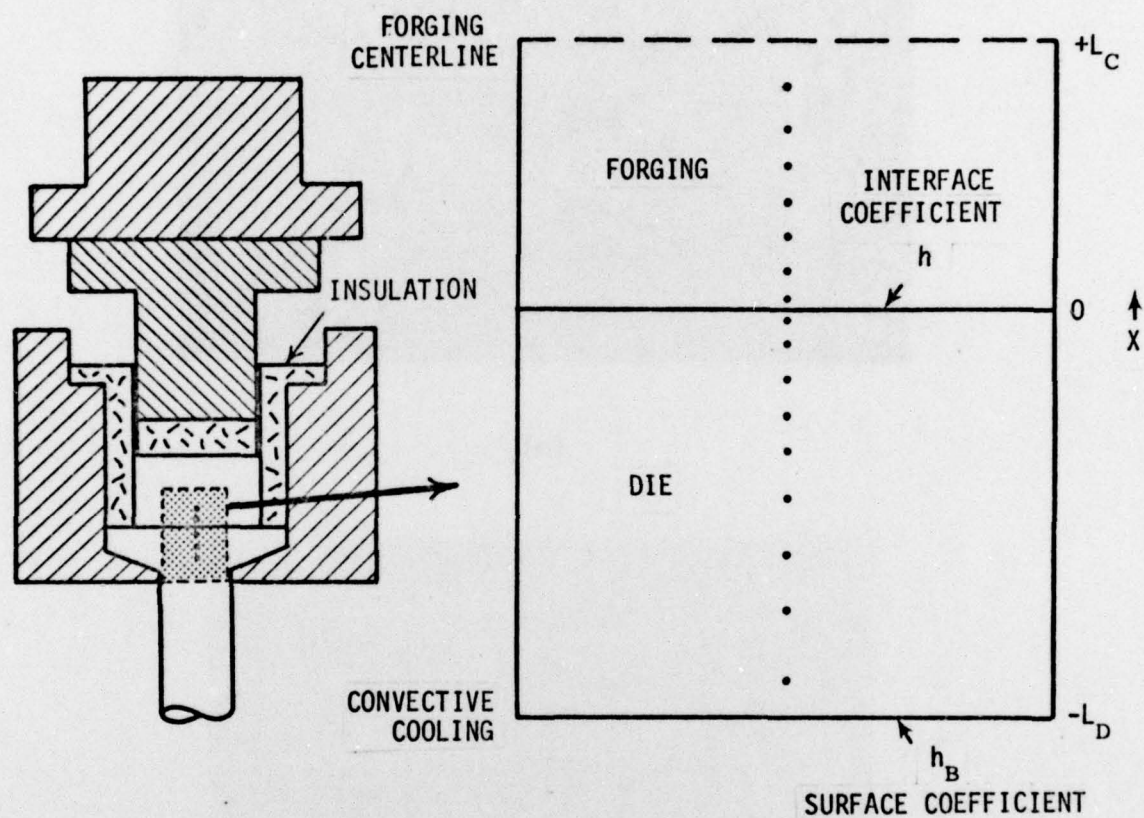


Figure 11. Schematic showing the volume element assumed to have a unidirectional thermal behavior. Expanded view shows positions of the nodes used in computer simulation studies.

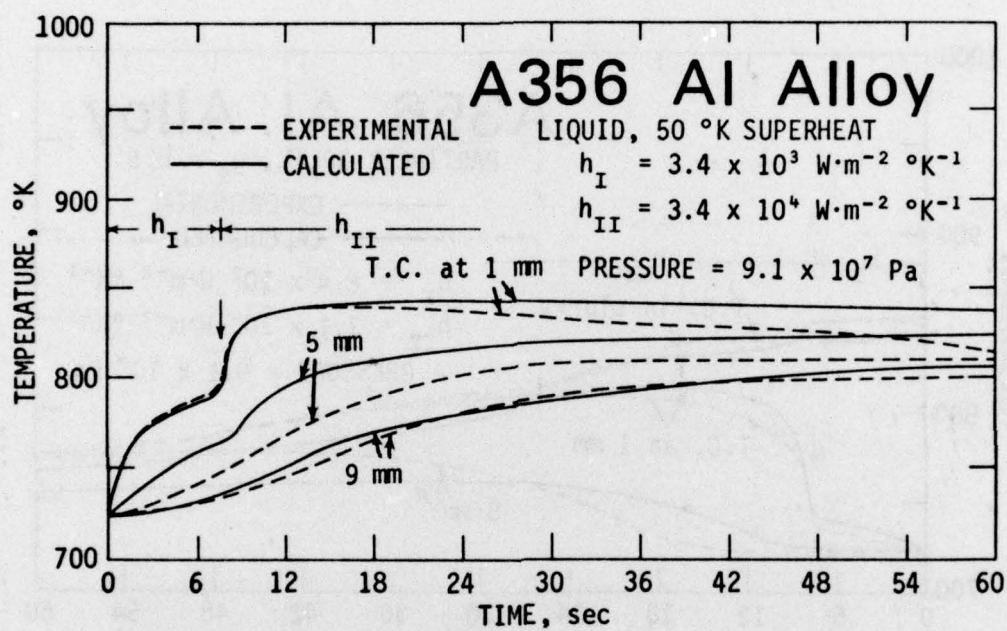


Figure 12. Die thermal response -- comparison between measured and calculated temperature profiles. Unidirectional die cavity.



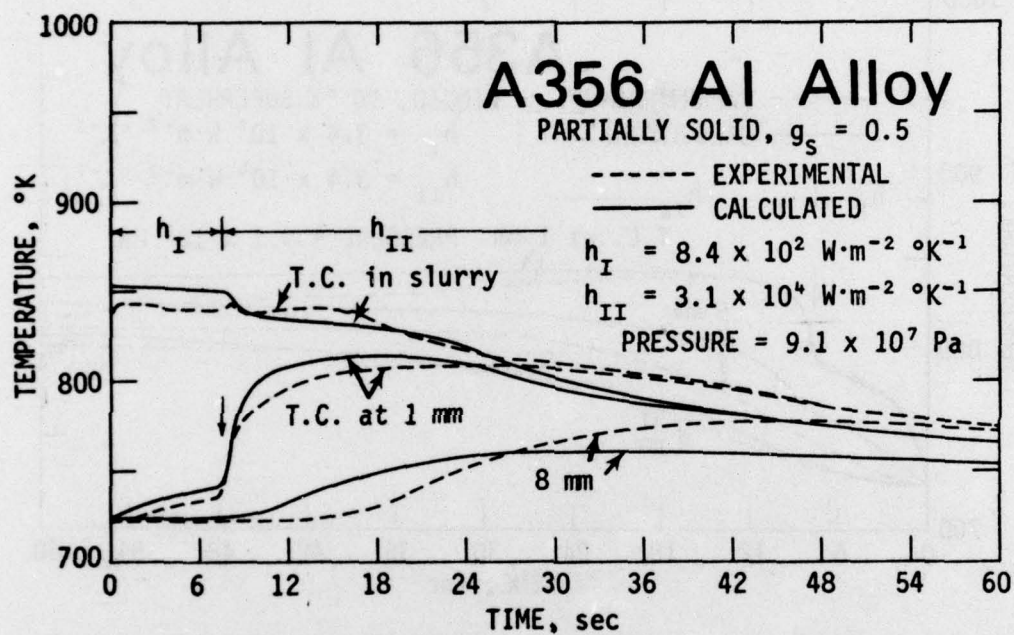


Figure 13. Composite of die and forging thermal responses -- comparison between measured and calculated temperature profiles. Unidirectional die cavity.

# DISTRIBUTION LIST

No. of Copies	To
1	Office of the Director, Defense Research and Engineering, The Pentagon, Washington, D. C. 20301
12	Commander, Defense Documentation Center, Cameron Station, Building 5, 5010 Duke Street, Alexandria, Virginia 22314
1	Metals and Ceramics Information Center, Battelle Columbus Laboratories, 505 King Avenue, Columbus, Ohio 43201
	Deputy Chief of Staff, Research, Development, and Acquisition, Headquarters, Department of the Army, Washington, D. C. 20310
2	ATTN: DAMA-ARZ
	Commander, Army Research Office, P. O. Box 12211, Research Triangle Park, North Carolina 27709
1	ATTN: Information Processing Office
	Commander, U. S. Army Materiel Development and Readiness Command, 5001 Eisenhower Avenue, Alexandria, Virginia 22333
1	ATTN: DRCLDC, Mr. R. Zentner
	Commander, U. S. Army Communications Research and Development Command, Fort Monmouth, New Jersey 07703
1	ATTN: DRDCO-GG-DD
1	DRDCO-GG-DM
1	DRDCO-GG-E
1	DRDCO-GG-EA
1	DRDCO-GG-ES
1	DRDCO-GG-EG
	Commander, U. S. Army Armament Research and Development Command, Dover, New Jersey 07801
2	ATTN: Technical Library
1	DRDAR-SCM, Mr. J. D. Corrie
1	DRDAR-SC, Dr. C. M. Hudson
1	DRDAR-PPW-PB, Mr. Francis X. Walter
	Commander, U. S. Army Natick Research and Development Command, Natick, Massachusetts 01760
1	ATTN: Technical Library
1	Dr. E. W. Ross
1	DRXNM-AAP, Mr. J. Falcone
	Commander, U. S. Army Satellite Communications Agency, Fort Monmouth, New Jersey 07703
1	ATTN: Technical Document Center

No. of Copies	To
	Commander, U. S. Army Tank-Automotive Research and Development Command, Warren, Michigan 48090
1	ATTN: DRDTA-RKA
2	DRDTA-UL, Technical Library
	Commander, White Sands Missile Range, New Mexico 88002
1	ATTN: STEWS-WS-VT
	Commander, Aberdeen Proving Ground, Maryland 21005
1	ATTN: STEAP-TL, Bldg. 305
	Commander, Frankford Arsenal, Philadelphia, Pennsylvania 19137
1	ATTN: Library, H1300, B1. 51-2
	Commander, Harry Diamond Laboratories, 2800 Powder Mill Road, Adelphi, Maryland 20783
1	ATTN: Technical Information Office
	Commander, U. S. Army Ballistic Research Laboratory, Aberdeen Proving Ground, Maryland 21005
1	ATTN: Dr. R. Vitali
1	Dr. G. L. Filbey
1	Dr. W. Gillich
	Commander, Picatinny Arsenal, Dover, New Jersey 07801
1	ATTN: SARPA-RT-S
1	SARPA-FR-M-D, PLASTEC, A. M. Anzalone
1	Mr. A. Devine
	Redstone Scientific Information Center, U. S. Army Missile Research and Development Command, Redstone Arsenal, Alabama 35809
4	ATTN: DRDMI-TBD
	Commander, Watervliet Arsenal, Watervliet, New York 12189
1	ATTN: SARWV-RDT, Technical Information Services Office
1	Dr. T. Davidson
1	Mr. D. P. Kendall
1	Mr. J. F. Throop
	Commander, U. S. Army Foreign Science and Technology Center, 220 7th Street, N. E., Charlottesville, Virginia 22901
1	ATTN: Mr. Marley, Military Tech
	Director, Eustis Directorate, U. S. Army Air Mobility Research and Development Laboratory, Fort Eustis, Virginia 23604
1	ATTN: Mr. J. Robinson, DAVDL-E-MOS (AVRADCOM)
1	Mr. R. Berresford



No. of Copies	To
1	U. S. Army Aviation Training Library, Fort Rucker, Alabama 36360 ATTN: Buildings 5906-5907
1	Commander, USACDC Air Defense Agency, Fort Bliss, Texas 79916 ATTN: Technical Library
1	Commander, U. S. Army Engineer School, Fort Belvoir, Virginia 22060 ATTN: Library
1	Commander, U. S. Army Engineer Waterways Experiment Station, Vicksburg, Mississippi 39180 ATTN: Research Center Library
1	Aeronautic Structures Laboratories, Naval Air Engineering Center, Philadelphia, Pennsylvania 19112 ATTN: Library
1	Naval Air Development Center, Aero Materials Department, Warminster, Pennsylvania 18974 ATTN: J. Viglione
1	David Taylor Naval Ship Research and Development Laboratory, Annapolis, Maryland 21402 ATTN: Dr. H. P. Chu
1	Naval Underwater Systems Center, New London, Connecticut 06320 ATTN: R. Kasper
1	Naval Research Laboratory, Washington, D. C. 20375 ATTN: Dr. J. M. Krafft - Code 8430
1	C. D. Beachem, Head, Adv. Mat'ls Tech Br (Code 6310)
1	Chief of Naval Research, Arlington, Virginia 22217 ATTN: Code 471
1	Naval Weapons Laboratory, Washington, D. C. 20390 ATTN: H. W. Romine, Mail Stop 103
1	Director, Structural Mechanics Research, Office of Naval Research, 800 North Quincy Street, Arlington, Virginia 22203 ATTN: Dr. N. Perrone
2	Air Force Materials Laboratory, Wright-Patterson Air Force Base, Ohio 45433 ATTN: AFML/MXE/E. Morrissey
1	AFML/LC
1	AFML/LLP/D. M. Forney, Jr.
1	AFML/MBC/Stanley Schulman
1	AFML/LNC/T. J. Reinhart

No. of  
Copies

To

Air Force Materials Laboratory, Wright-Patterson Air Force Base, Ohio 45433  
1 ATTN: AFFDL (FB), Dr. J. C. Halpin  
1 Dr. S. Tsai  
1 Dr. N. Pagano

Air Force Flight Dynamics Laboratory, Wright-Patterson Air Force Base,  
Ohio 45433  
1 ATTN: AFFDL (FBS), C. Wallace  
1 AFFDL (FBEB), G. D. Sendekyj

National Aeronautics and Space Administration, Washington, D. C. 20546  
1 ATTN: Mr. B. G. Achhammer  
1 Mr. G. C. Deutsch - Code RW

National Aeronautics and Space Administration, Marshall Space Flight  
Center, Huntsville, Alabama 35812  
1 ATTN: R. J. Schwinghamer, EH01, Director, M&P Laboratory  
1 Mr. W. A. Wilson, EH41, Building 4612

National Aeronautics and Space Administration, Langley Research Center,  
Hampton, Virginia 23365  
1 ATTN: Mr. H. F. Hardrath, Mail Stop 188M  
1 Mr. R. Foye, Mail Stop 188A

National Aeronautics and Space Administration, Lewis Research Center,  
21000 Brookpark Road, Cleveland, Ohio 44135  
1 ATTN: Mr. S. S. Manson  
1 Dr. J. E. Srawley, Mail Stop 105-1  
1 Mr. W. F. Brown, Jr.

National Bureau of Standards, U. S. Department of Commerce,  
Washington, D. C. 20234  
1 ATTN: Mr. J. A. Bennett

Virginia Polytechnic Institute and State University, Dept. of Engineering  
Mechanics, 230 Norris Hall, Blacksburg, Virginia 24061  
1 ATTN: Prof. R. M. Barker

Southwest Research Institute, 8500 Culebra Road, San Antonio, Texas 78284  
1 ATTN: Mr. G. C. Grimes

Westinghouse Electric Company, Pittsburgh, Pennsylvania 15235  
1 ATTN: Mr. E. T. Wessel, Research and Development Center

1 Mr. M. J. Manjoine, Westinghouse Research Laboratory, Churchill Boro,  
Pittsburgh, Pennsylvania 15235

1 Mr. William J. Walker, Air Force Office of Scientific Research,  
1400 Wilson Boulevard, Arlington, Virginia 22209

No. of  
Copies

To

- |   |                                                                                                                                                           |
|---|-----------------------------------------------------------------------------------------------------------------------------------------------------------|
| 1 | Mr. Elmer Wheeler, Airesearch Manufacturing Company, 402 S. 36th Street,<br>Phoenix, Arizona 85034                                                        |
| 1 | Mr. Charles D. Roach, U. S. Army Scientific and Technical Information Team,<br>6000 Frankfurt/Main, I.G. Hochhaus, Room 750, West Germany (APO 09710, NY) |
|   | Director, Army Materials and Mechanics Research Center,<br>Watertown, Massachusetts 02172                                                                 |
| 2 | ATTN: DRXMR-PL                                                                                                                                            |
| 1 | DRXMR-PR                                                                                                                                                  |
| 1 | DRXMR-X                                                                                                                                                   |
| 1 | DRXMR-CT                                                                                                                                                  |
| 1 | DRXMR-AP                                                                                                                                                  |
| 3 | DRXMR-EM, Dr. R. French                                                                                                                                   |
| 3 | DRXMR-ER, Mr. F. Quigley                                                                                                                                  |
| 3 | DRXMR-ER, Mr. R. Gagne                                                                                                                                    |



